Strong Reduction in Amplitude of the Interfacial Segmental Dynamics in Polymer Nanocomposites

Ivan Popov[1], Bobby Carroll[2], Vera Bocharova[1], Anne-Caroline Genix[4], Shiwang Cheng[5], Airat Khamzin[6], Alexander Kisliuk[1], Alexei P. Sokolov[1,3]*

[1]Chemical Sciences Division, Oak Ridge National Laboratory, Oak Ridge, Tennessee 37831, USA

[2]Department of Physics, University of Tennessee, Knoxville, Tennessee 37996, USA

[3]Department of Chemistry, University of Tennessee, Knoxville, Tennessee 37996, USA

[4]Laboratoire Charles Coulomb, Université de Montpellier, CNRS, F-34095, France

[5]Department of Chemical Engineering and Materials Science, Michigan State University, East Lancing, Michigan 48824, USA

[6]Kazan Federal University, Institute of Physics, 420008, Kremlevskaya str.18, Kazan, Tatarstan, Russia

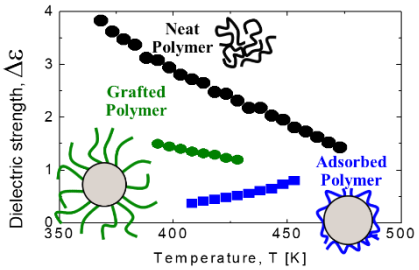

Abstract

Despite wide use of polymer nanocomposites (PNCs) in various applications, our understanding of microscopic parameters controlling their macroscopic properties remains limited. In this study, we examine the dielectric strength of segmental dynamics $\Delta\varepsilon_{IL}(T)$ in the interfacial polymer layer surrounding nanoparticles in PNCs. The presented analysis reveals significant drop in $\Delta\varepsilon_{IL}(T)$, and its anomalous temperature dependence in polymer layer adsorbed to nanoparticles. The drop in $\Delta\varepsilon_{IL}(T)$ was observed in all samples regardless whether segmental relaxation time in the interfacial layer was slower or faster than in the bulk polymer, excluding interpretation of the 'dead' layer. We ascribe the observed decrease in the dielectric strength to the restricted amplitude of segmental relaxation in the interfacial/adsorbed layer. Our results provide new perspective on discussion of dynamics in the interfacial layer in PNCs and thin polymer films, demonstrating that not only segmental relaxation time but also its amplitude can be strongly affected by the interface.

Keywords: Polymer nanocomposite; interfacial layer; dielectric properties, segmental dynamics, grafted nanoparticles, thin polymer films

Introduction

Polymer nanocomposites (PNCs) with nanoscale fillers dispersed in a polymer matrix are widely used in many applications and have generated extensive research interest in materials science [1-19]. This interest is caused by a wide range of macroscopic properties that can be achieved in PNCs. It becomes clear that the interfacial layer formed around nanoparticles plays a critical role in defining these macroscopic properties[17]. The thickness of the interfacial layer in PNCs is usually in the range ~2-6 nm[17, 20-25]. Interfacial layer is also formed in polymers confined to nanopores [26] and in

thin polymer films [27-44]. It was shown that characteristic structural (segmental) relaxation time in the interfacial layer might differ significantly from that in the neat polymer [20, 31, 34, 38, 40-41, 43, 45-51], it can be faster or slower depending e.g. on polymer – nanoparticle (or substrate) interactions. Also mechanical properties in the interfacial layer differ significantly from that of the bulk polymer, leading to substantial mechanical reinforcement of PNCs [6, 14, 46, 52-53].

In current literature interfacial layer sometimes is confused with the bound polymer layer. Bound layer (see Sketch 1) is formed by the molecules adsorbed at the interface, and its thickness is usually comparable to the radius of gyration (Rg) of the adsorbed molecules [46-51, 54-56] (unless the distance to another interface is smaller than Rg). Bound layer is formed in solution and might depend on the solution used [57]. The bound layer in PNCs provides repulsion between nanoparticles at higher loading and helps to improve their dispersion [46, 50]. It also slows down diffusion of nanoparticles in polymer melt by increasing their hydrodynamic radius [54, 58]. Although it was shown that estimates of the bound layer thickness might depend on the method used[50], it is generally accepted that the thickness of the bound layer (non-confined between interfaces) increases with the molecular weight (MW) of the polymer[50, 54].

The interfacial layer is defined as the region with the properties of the polymer changed by the presence of the interface (see Sketch 1). These can be changes in density, segmental relaxation time, mechanical properties, etc. [20, 24, 28, 34, 38, 52-53, 59-60]. In contrast to the bound layer, the thickness of the interfacial layer shows no significant dependence on molecular weight [45, 53], but it increases with chain stiffness and upon cooling [17, 20-25]. It has been also shown that the thickness of the interfacial layer decreases with the decrease in nanoparticles size [61] (although authors called it bound layer).

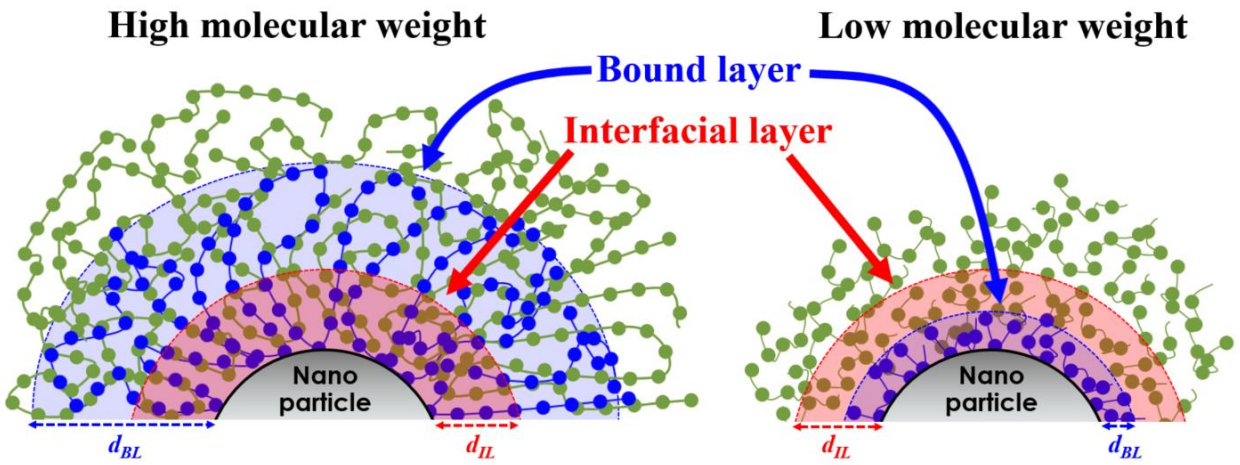

Sketch 1. Difference between the bound and the interfacial layer. The bound layer is formed by adsorbed (blue) chains and its thickness, d_{BL}, increases with polymer MW, while interfacial layer is formed by adsorbed and free (green) chains, and presents the polymer region with properties affected by the presence of the interface. Its thickness, d_{IL}, is essentially MW independent, and increases with chain rigidity and upon cooling[17, 20-25].

In many PNCs and thin polymer films, the interfacial layer shows segmental relaxation significantly slower than in the bulk polymer[20, 24, 28, 34, 38, 53, 59]. One of the best techniques to study the segmental dynamics in these systems is the Broadband Dielectric Spectroscopy (BDS) [20, 34, 36, 62-65]. Advantages of BDS are extremely broad frequency range (more than 10 decades) and very high accuracy. It has been noticed that the segmental peak in the dielectric spectra of PNCs broadens on the low-frequency side, and decreases in amplitude stronger than expected from the polymer volume fraction [25, 61, 66] The authors of study [61] ascribed this lost amplitude of the bulk-like dielectric response to the 'segments immobilized in the bound layer". However, more detailed analysis of the dielectric spectra revealed that the segments in the interfacial layer are not immobilized, but slowed down significantly, leading to the additional dielectric response at lower frequencies [25, 61]. MD simulations of PNCs and thin films also revealed a gradient of segmental

relaxation time in the interfacial layer, but no frozen or immobilized segments [67-70]. Recent analysis of bound layer in PNC using small angle neutron scattering and partially deuterated polymer[49] reveals significant exchange of the adsorbed and free chains, again emphasizing that the adsorbed chains remain mobile, although slowed down significantly.

Many earlier BDS studies provided critical information on dynamics of the interfacial layer [20, 34, 62-65, 71]. These PNCs studies were traditionally focused on explanation of changes in characteristic segmental relaxation time of the interfacial layer $\tau_{IL}(T)$, while not much attention has been paid to analysis of the dielectric strength of segmental dynamics in the interfacial layer, $\Delta\varepsilon_{IL}(T)$. Detailed studies of thin polymer films revealed significant reduction of the dielectric strength of segmental relaxation [28-31, 33-44]. It was demonstrated that regardless of whether segmental dynamic in thin films is getting faster or slower than in the bulk polymer (i.e. the glass transition temperature Tg decreases or increases), segmental $\Delta\varepsilon$ always decreases [28-31, 33-44]. As we mentioned above, a decrease of the amplitude of the bulk-like segmental peak in the dielectric spectra of PNCs, $\Delta\varepsilon$, has also been noticed earlier [28-31, 33-34, 36-44, 66]. This decrease, however, was assigned to segments in the interfacial layer that might contribute to the dielectric spectra at lower frequency. There are only a few papers that analyzed the dielectric strength of segmental relaxation $\Delta\varepsilon_{IL}(T)$ in the interfacial layer in PNCs[20, 66, 72-73]. They all revealed a significant decrease in the dielectric strength of the interfacial layer. One of the obvious ideas proposed to explain this effect is the 'dead layer' model, [39, 43, 74] implying that the significant fraction of segmental dipoles being frozen and not contributing to the dielectric response. The idea of 'dead' (or glassy) layer has been widely used in many studies to explain various experimental results in PNCs and thin polymer films [27, 39, 66, 74-76]. However, as was mentioned above, there are many experimental and simulations data that contradict the idea of 'dead' layer and emphasize that the dynamics in the interfacial layer is not

frozen, although can be much slower than in the bulk [20-21, 25, 45, 59]. Thus, the suppression of the dielectric strength of segmental dynamics in the interfacial layer might have different mechanism, and its understanding can provide additional critical information on properties of the interfacial layer, and might have fundamental implications for the fields of PNCs and thin films.

This article focuses on analysis of the dielectric strength of segmental relaxation, $\Delta\varepsilon_{IL}(T)$, in the interfacial layer in various types of PNCs. We specifically chose a well-studied model system - poly(2-vinyl pyridine) (P2VP) with silica nanoparticles. We used nanoparticles with grafted polymer chains (GNP), regular PNC and nanoparticles with only adsorbed polymer layer (APL). The latter system is the PNC where polymer chains non-adsorbed and weakly adsorbed to nanoparticles (NP) were removed by centrifugation. Thus, only strongly adsorbed polymer chains remains in the APL samples. In all cases, we found significant decrease in the dielectric strength of segmental dynamics in the interfacial/adsorbed layer. Interestingly, however, $\Delta\varepsilon(T)$ in APL shows anomalous temperature dependence: It decreases with cooling, while in neat polymer and GNP the $\Delta\varepsilon(T)$ increases with cooling (normal Curie law). At the same time, the average segmental relaxation time in the adsorbed layer does not differ significantly from that of neat polymers. We ascribe the observed changes in $\Delta\varepsilon(T)$ to the restriction of the amplitude of segmental motions in the interfacial layer. We propose a simple model that explains the observed results without involving 'dead' layer.

Material and Methods

Adsorbed Polymer Layer samples: To focus on the dielectric response of a polymer in the nanoparticles vicinity, we prepared samples of nanoparticles with only adsorbed polymer layer (APL), where not adsorbed or weakly adsorbed chains were removed. We choose the well-studied

P2VP/silica nanocomposites as a model system. P2VP with molecular weights (MW) 9kg/mol, 36kg/mol, 101kg/mol, and 400kg/mol were purchased from Scientific Polymer Products. Monodisperse colloidal silica nanoparticles (D = 20 nm) were synthesized by the modified Stöber method according to previous reports [77-78]. In order to prepare the APL samples, a polymer and nanoparticles were dissolved in ethanol and spun overnight. Then, the solution was centrifuged in 2mL vials for one hour. The solution (containing the free P2VP polymer) at the top of the vial was removed and the precipitate (nanoparticles with adsorbed polymer) at the bottom was re-dissolved in ethanol via sonication for 10-15 min. This procedure was repeated twice, meaning the sample was centrifuged 3 times. After the final centrifugation, the precipitate was removed from the vials and allowed to dry in a Teflon dish overnight. To remove any remaining solvents, the samples were annealed at 120°C in vacuum for at least one week prior to measurements.

Thermogravimetric analysis (TGA) was employed to estimate the weight fraction of nanoparticles in the samples. The samples were heated in air to 900°C at a rate of 20°C/min using a Discover Q50 instrument (Fig. S1 in SM). The level reached at T ~ 800C was used to estimate the weight fraction of silica nanoparticles.

Broadband Dielectric Spectra (BDS) were measured in the frequency range of 10^{-2} −10^{7} Hz, using a Novocontrol Concept-80 system with Alpha-A impedance analyzer. Temperature was controlled by a Quatro Cryosystem with a stability of ±0.1 K. All samples were measured between two gold-coated electrodes. The APL samples did not form a good stable film in a hot press, and were measured as a pressed powder. The samples were equilibrated for 20 minutes at each T prior to the measurements. Measurements started at the highest temperature, and the cooling was done in 5°C steps.

Result and Discussion

Thermogravimetric analysis (TGA) data of APL samples (Fig. S1 in Supplementary Materials (SM)) reveals that the mass fraction of the adsorbed polymer increases from ~25wt% for lowest molecular weight polymer to ~40wt% in the highest MW sample (Fig. 1). Using the obtained weight fraction of the silica particles, ϕ_{NP}^{m}, their radius $R_{NP} = 10\,\text{nm}$, and density $\rho_{NP} = 2.45\ \text{g/cm}^3$, and assuming that the polymer forms a homogenous layer around nanoparticle with the density of the bulk polymer ρ_{polymer}, we can estimate the expected thickness of the adsorbed layer (Fig. 1)

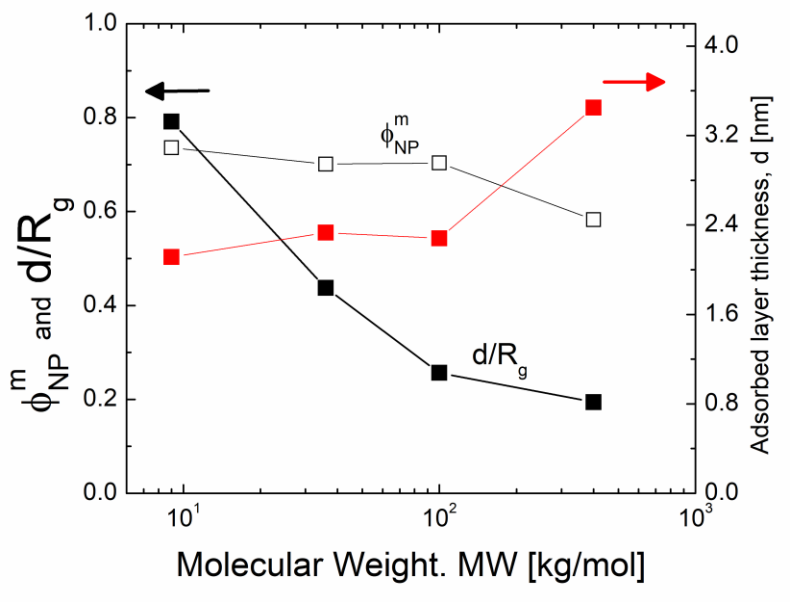

Figure 1. Weight fraction of nanoparticles in the APL samples, ϕ_{NP}^{m}, (black open squares); expected adsorbed layer thickness (red full squares) and ratio d/R_g (black full squares) calculated from the Eq. (1).

$$d = R_{NP}\left[\left(1 + \frac{1-\phi_{NP}^{m}}{\phi_{NP}^{m}}\frac{\rho_{NP}}{\rho_{polymer}}\right)^{1/3} - 1\right]. \qquad (1)$$

The analysis suggests (Fig. 1) that the expected thickness of the adsorbed layer is ~2-3.5 nm and increases slightly with MW, while its ratio to polymer radius of gyration, d/R_g, decreases sharply with MW suggesting formation of pancake-like structure. We emphasize that the estimated d is not the real thickness of the adsorbed layer, because most probably the polymer density in this layer is significantly lower than in the bulk, especially for higher MW samples. Thus, the thickness presented in the Fig 1 is the lower estimate of the adsorbed layer thickness.

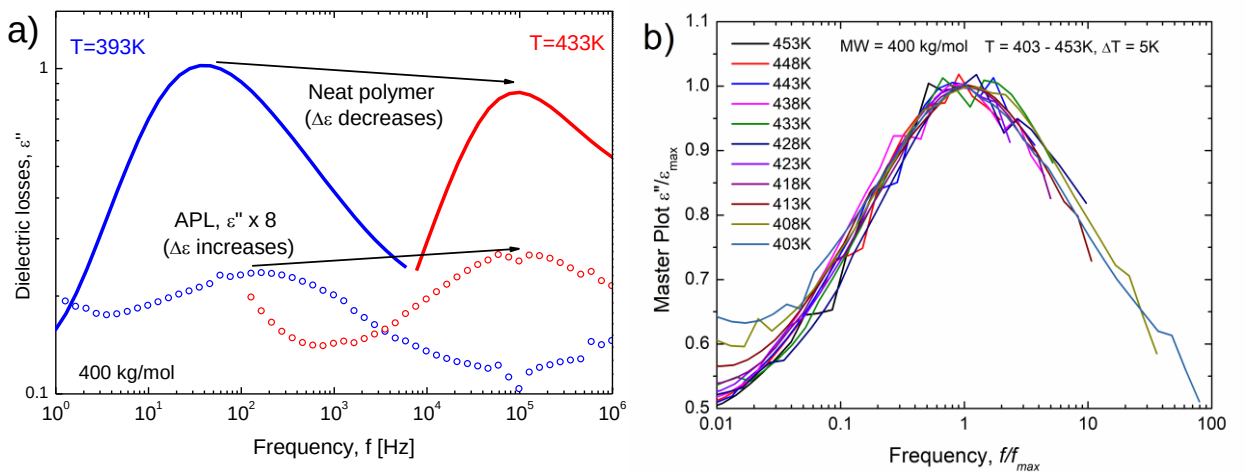

Figure 2. a) Dielectric loss spectra of neat P2VP (lines) and APL samples (symbols) with MW=400kg/mol at T=393K (blue) and T=433 K (red). For convenience, the spectra of APL sample are multiplied by a factor of 8. **b)** Master plot of the dielectric losses for segmental relaxation in APL sample with MW = 400kg/mol reveals no significant change in the peak shape with temperature.

Broadband Dielectric Spectroscopy measurements were made in a wide temperature range from 313K up to 453K. The data measured on cooling and heating show good reproducibility, emphasizing no aging or other effects occur during the measurements. We note that the absence

of changes on heating and cooling does not exclude that the samples are in some none-equilibrium state. They might be in a deep metastable state that does not change even on time scale ~10^{10} times longer than characteristic segmental relaxation time. Analysis of the dielectric response of segmental relaxation in adsorbed polymer layer reveals two important results (Fig. 2a): (i) significant (~30 times) drop in the amplitude of segmental peak, when the weight fraction of the polymer is still ~40%; and (ii) surprising decrease of the amplitude upon cooling, while neat polymer exhibits the typical increase upon cooling (the Curie law). The spectrum of segmental relaxation in adsorbed layer appears extremely broad (Fig. 2, and Fig. S2 in SM) reflecting broad distribution of relaxation times. The latter is caused by a gradient in segmental dynamics with slower dynamics at the nanoparticle surface and faster dynamics at the free surface of the adsorbed layer. However, the shape of the peak in the APL systems shows no significant changes with temperature (Figure 2b).

To provide a quantitative analysis, the dielectric spectra were fit to a single Havriliak-Negami function, conductivity term and Jonsher's correction of the low frequency part [62]

$$\varepsilon^*(\omega) = \varepsilon_\infty + \frac{\sigma_0}{i\omega\varepsilon_0} + \frac{A}{(i\omega)^n} + \frac{\Delta\varepsilon}{\left[1+(i\omega\tau)^\alpha\right]^\beta}. \qquad (2)$$

Analysis of the fit results reveals that the characteristic relaxation time of segmental dynamics in APL samples estimated from the peak position, $\tau_{max} = \tau\left[\sin\left(\frac{\alpha\beta\pi}{2(1+\beta)}\right)\right]^{\frac{1}{\alpha}}\left[\sin\left(\frac{\alpha\pi}{2(1+\beta)}\right)\right]^{-\frac{1}{\alpha}}$, is comparable or even faster than in the neat polymer (Fig. 3a and Fig. S2 in SM). This is in contrast to the segmental relaxation in PNC and GNP samples, where it is usually slower than in the neat samples (Fig. 3) [23-25, 61, 64, 75]. Thus, acceleration of segmental dynamics in polymer adsorbed to an

attractive surface is unusual, but has been reported earlier for poly(propylene glycol) (PPG) adsorbed to silica nanoparticles [79], for PMMA/silica PNCs[80], for PMMA/Ag PNCs[81] and in thin polymer films[29, 40-41, 44]. In our case, this effect is more pronounced for higher molecular weight systems (Fig. 3a). In earlier papers[80-82] the counter-intuitive acceleration of segmental dynamics was ascribed to additional free volume in these systems. Following the same idea, we ascribe the observed effect to a frustration in packing of long chains in the adsorbed layer that creates extra free volume and accelerates segmental dynamics.

The most intriguing result, however, is the strong decrease in the amplitude of segmental peak in BDS spectra of the interfacial/adsorbed layer and its anomalous temperature dependence (Figs. 2a and 3c). The dielectric strength of interfacial/adsorbed layer $\Delta\varepsilon_{\mathrm{IL}} = \Delta\varepsilon_{\mathrm{Ads}}/(1-\phi_{NP}^{m})$ in APL systems is roughly 5-10 times lower than in the neat polymers, and it decreases upon cooling for all molecular weights (Fig. 3c). To broaden the analysis, we also include our earlier published data for P2VP-based PNC from [45, 53] and GNP from [24], and for poly(vinyl acetate) (PVAc) based PNC from [45]. In the data analysis, in the case of short (MW~6kg/mol) grafted P2VP chains the entire polymer fraction was considered as the interfacial layer [24], while analysis of the interfacial layer spectra in PNCs was done using the Interfacial Layer Model [20, 45]. Analysis of BDS data reveals a significant slowdown of the segmental dynamics in GNP and PNCs (Figs. 3a, 3b). However, $\Delta\varepsilon_{\mathrm{IL}}$(T) of the interfacial layer in PNCs is suppressed as strongly as in APL samples (Figs. 3c, 3d), while $\Delta\varepsilon_{\mathrm{IL}}$(T) in GNP shows the behavior in between those of the neat and adsorbed polymers (Figs. 3c). Thus, regardless of whether average interfacial segmental dynamics is getting slower (GNP and PNC), remains nearly the same or even accelerates (APL), the dielectric strength of the interfacial segmental dynamics is always suppressed (Fig. 3). These results are similar to the earlier observations in thin polymer films where segmental $\Delta\varepsilon$ always decreases with decrease in film

thickness, regardless whether the film T_g increases or decreases (i.e. segmental dynamics slow down or accelerate) [28-31, 33-44].

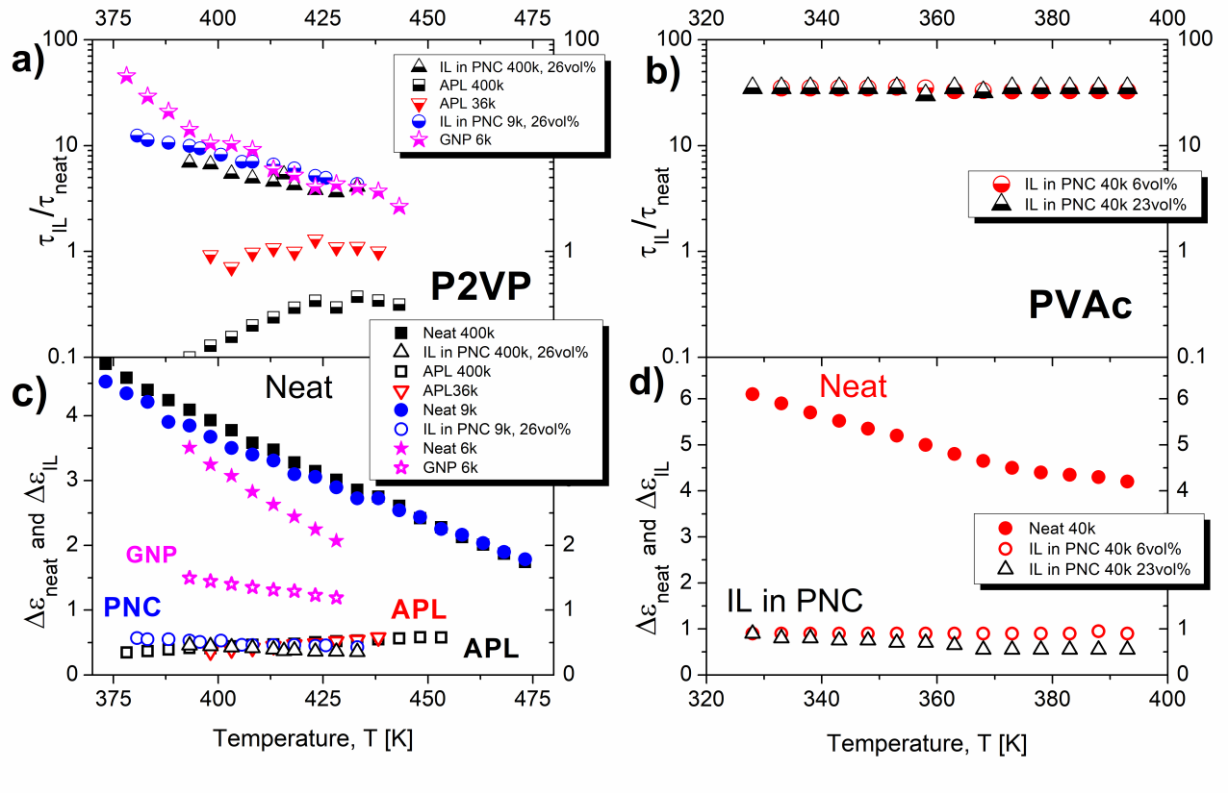

Figure 3. (**a, b**) Temperature dependence of the ratio of the segmental relaxation times (half-filled symbols) in the interfacial/adsorbed layer (IL), τ_{IL}, to that in the neat polymer, τ_{neat}. (**c**, **d**) Temperature dependence of the dielectric strength of the neat polymer, $\Delta\varepsilon_{neat}$ (closed symbols), and of the interfacial/adsorbed layer, $\Delta\varepsilon_{IL}$ (open symbols). **a)** and **c**) present the data for neat P2VP and APL samples with MW=400kg/mol (black squares); 36kg/mol (red down triangles) and 9kg/mol (blue circles). P2VP PNC data are from [53]. Magenta stars present data for GNP and neat polymer with MW=6kg/mol (data from [24]). **b)** and **d)** present the data for neat PVAc with MW=40kg/mol and for the interfacial layer in PVAc-based PNC with 2 different nanoparticle loadings estimated using Interfacial Layer Model, data from [20, 45].

Thus, the decrease in the dielectric strength of the segmental peak is a general behavior for the interfacial layers in PNC, GNP, adsorbed polymer layer, and thin polymer films. What is the origin of this suppression in the dielectric signal? In a simple approximation, neglecting Onsager local electric field corrections and presenting polymer chain as a set of segmental dipoles, the relative dielectric strength of polymer can be described as [83]

$$\Delta\varepsilon_{neat} = \frac{N\bar{\mu}}{VE} = \frac{gN\mu^2}{3k_BTV}, \quad (3)$$

where N is the number of dipoles per volume V, μ is the segmental dipole moment and g is the Kirkwood-Fröhlich factor that accounts for dipole-dipole correlations. The decrease of $\Delta\varepsilon$ in thin films was interpreted as a decrease in the number of participating dipoles N in comparison to the neat polymer, i.e. to the so-called 'dead layer'[31, 34, 39, 43, 74]. A similar interpretation was recently proposed for the description of the reduced $\Delta\varepsilon_{IL}$ in PNC [66]. It has been shown, however, that in the case of many PNCs there is no significant 'dead' layer, and segmental dynamic just slows down [21, 25, 45]. The observed acceleration of average segmental dynamics in APL (Fig. 3) also seems contradictory to the idea of the dead layer. Moreover, our results reveal that although interfacial segmental dynamics in GNP is significantly slower than in APL (Fig. 3a), the decrease in the dielectric strength in GNP is much weaker (Fig. 3c). These observations reveal a very important property of the dynamics in the interfacial layer: *behavior of segmental relaxation time and segmental relaxation amplitude in the interfacial layer can differ strongly*. Furthermore, no significant change in the spectral shape of the segmental peak in APL with temperature (Fig. 2b) excludes a possibility of unfreezing the 'dead' layer with temperature as the major reason for the observed temperature changes in $\Delta\varepsilon(T)$. Indeed, a significant additional broadening would be expected on the low-frequency side of the segmental peak with 'unfreezing' dipoles from the dead

layer. No this low frequency broadening has been observed in the experiment. Thus, there are several results contradicting to the idea ascribing the reduction of Δε to the 'dead' layer in PNC. Alternative explanation can relate the observed changes in Δε to the constrained amplitude of segmental relaxation caused by specific chain conformations in the interfacial layer and segmental dipole's correlation. To the best of our knowledge, this scenario has not been discussed in literature.

It is important to emphasize that earlier analysis of the dielectric strength in the interfacial layer of glycerol/silica composites revealed no significant change in the amplitude Δε [20, 84]. Glycerol molecules are small and there is no particular restrictions on the amplitude of their reorientation in the interfacial layer, their dynamics just slow down [20, 84]. This result emphasizes importance of the chain connectivity and specific role of chain conformations in the interfacial layer in restricting the amplitude of segmental Δε(T). The chains are expected to be stretched in the interfacial layer in GNP and PNC [52, 85]. As a result, the reorientation of the segments (and of the associated dipoles) is limited on the segmental time scale. This time scale might not differ much from the segmental relaxation time of the neat polymer due to competing effects of the chain adsorption, stretching and packing (density) [24, 52-53]. However, the amplitude of the dielectric strength will be strongly suppressed due to the restricted amplitude of segmental reorientation. The most probable chain conformation in the adsorbed polymer layer, especially at high MW, is a pancake-like structure [86-87]. The amplitude of the segmental reorientation will be also limited in the pancake-like structure, especially in the out-of-plane direction. This idea of restricted segmental amplitude in the interfacial layer is supported by recent Neutron Spin Echo studies of GNP [88], where it was found that the intermediate scattering function associated with the relaxation of grafted chains does not decay completely to zero. Instead, there is a non-relaxing part that depends on the scattering wave-

vector Q, similar to the behavior of confined diffusion with confinement length defined by the polymer grafting density [88]. Non-relaxing part of the intermediate scattering function was also observed in the (NSE) studies of solutions of polybutadiene chains adsorbed to carbon black nanoparticles [48].

Restricted amplitude of segmental relaxation in the interfacial layer leads to a limited angle of the dipole reorientation. To describe this restriction theoretically, one needs to introduce a specific potential for the angle of the dipole (segment) reorientation, and this potential should have a gradient changing with the distance from the interface. Thus, a detailed microscopic description of this effect presents significant theoretical challenge. Instead, we use a simple assumption that segments can freely fluctuate in a conical angle 2δ, but any larger angle reorientation requires to overcome a fixed potential energy barrier *U* (cartoon in Fig. 5b and Fig.S3). In this case we can rewrite Eq.(3)

$$\Delta\varepsilon_{\mathrm{Ads}} = (1-\phi_{NP}^{m})\frac{N\bar{\mu}_{Ads}}{VE} = (1-\phi_{NP}^{m})\frac{gN}{VE}\langle\mu\overline{\cos\theta}\rangle_{NP}, \quad (4)$$

where $\langle\dots\rangle_{NP}$ defines an averaging of the potential wells around nanoparticle and $\overline{\cos\theta}$ is an averaging of the angle between the dipole moment and the electrical field inside the potential well

$$\overline{\cos\theta} = \int \cos(\widehat{\mathbf{E}\boldsymbol{\mu}})\, e^{\frac{(\mathbf{E}\boldsymbol{\mu})-U}{k_BT}}\, d\Omega / \int e^{\frac{(\mathbf{E}\boldsymbol{\mu})-U}{k_BT}}\, d\Omega. \quad (5)$$

Thus, instead of changing the numbers of the dipole moments, *N*, as assumed in the 'dead layer' model, we introduce the restricted amplitude of the dipole reorientation caused by interactions between stretched neighbor chains. In usual unrestricted case (Eq. (3)), contribution of each dipole is proportional to μ^2 (neglecting dipole-dipole correlations). Restriction of the dipole reorientation angle leads to a decrease of the dielectric signal produced by each dipole (Eqs. (4) and (5)), and is

controlled by average $\overline{\cos\theta}$. The calculation of (5) (for details see SM), assuming that $\mu E/k_BT << 1$ (usual conditions for BDS experiment), provides simple relationship

$$\Delta\varepsilon_{\mathrm{IL}} = \frac{\Delta\varepsilon_{\mathrm{Ads}}}{(1-\phi_{NP}^{m})} = \frac{gN\mu^2}{3k_BTV}(1-f^2), \quad f = \frac{\sin^2\delta}{2(\coth(U/2k_BT)-\cos\delta)}, \tag{6}$$

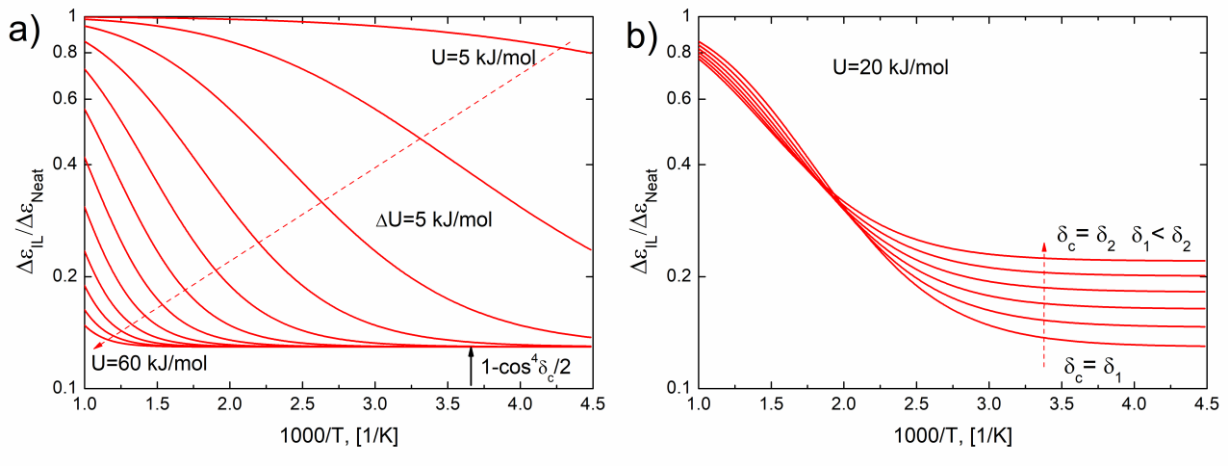

Figure 4. The model data obtained from the Eq.7 for different value of potential barrier U **(a)** and angle δ **(b)**

Using the definition of $\Delta\varepsilon_{Neat} = gN\mu^2/3k_BTV$, we can write

$$\frac{\Delta\varepsilon_{\mathrm{IL}}}{\Delta\varepsilon_{Neat}} = \frac{\Delta\varepsilon_{Ads}}{\Delta\varepsilon_{Neat}(1-\phi_{NP}^{m})} = \left(1-f^2\right) \tag{7}$$

Predictions of the model Eq.(7) in a wide temperature range for different values of potential barrier U and angle δ are presented in the Figures 4a and 4b.

In the limit of high temperatures ($U \ll k_BT$), we have $f \to 0$, and the Eq.(7) reduces to the classical result Eq.(3), i.e. $\Delta\varepsilon_{\mathrm{IL}} \to \Delta\varepsilon_{\mathrm{neat}}$. In contrast, in the case of $U/k_BT \gg 1$, Eq.(7) predicts a temperature independent behavior for the ratio $\Delta\varepsilon_{\mathrm{IL}}/\Delta\varepsilon_{\mathrm{neat}} = 1 - cos^4[\delta/2]$ (Fig. 4). At small δ this ratio will be significantly smaller than 1, emphasizing that the dielectric response can be

strongly suppressed without decreasing the number of contributing dipoles. In the intermediate case, the Eq. (7) may be approximated by

$$\frac{\Delta\varepsilon_{\mathrm{IL}}}{\Delta\varepsilon_{\mathrm{Neat}}} \sim exp\left(-\frac{U}{k_B T}\right). \quad (8)$$

Analysis of the experimental data (Fig. 5a) indeed revealed that the ratio $\Delta\varepsilon_{IL}/\Delta\varepsilon_{neat}$ in PNCs is essentially T independent, corresponding to the case $U/k_BT \gg 1$. Moreover, the temperature dependence of the ratio for the APL, GNP and PVAc-based PNC at low loading follows well the Arrhenius dependence Eq.(8) (Fig. 5a). The latter provides estimate of the potential energy barrier *U*, which decreases with molecular weight of the adsorbed polymer (Fig. 5b). This decrease might be caused by the lower density of longer polymer chains adsorbed to nanoparticles that imposes less restrictions on reorientation of segments. Even smaller activation energy appears for grafted chains and for the interfacial layer in PNC with only 6vol% of nanoparticles (Fig. 5b). This result emphasizes that chain stretching in GNP and PNC with low nanoparticles loading imposes weaker restrictions on amplitude of segmental reorientation than the pancake-like structure in APL. However, when chain in PNC is confined between NPs, i.e. when the distance between NP surfaces is smaller than 2Rg of the chains (the case for both P2VP-based PNCs with ~26vol% [53] and for PVAc-based PNC with 23vol% of NPs [20, 45]), the energy barrier for softening of the segmental reorientation is much higher. The latter leads to temperature independent $\Delta\varepsilon_{IL}/\Delta\varepsilon_{neat}$. We want to emphasize that according to the proposed model, temperature independent $\Delta\varepsilon_{IL}/\Delta\varepsilon_{neat}$ does not mean $U = 0$, but corresponds to a very high potential barrier $U >> k_BT$ (see Figure 4a).

APL samples present especially interesting case (Figs. 3 and 5). Although the nanoparticles loading in APLs is high, the density of the adsorbed layer should be lower in comparison to PNCs. This density should decrease with increasing of molecular weight due to larger frustration in

packing of longer adsorbed chains. Lower density (higher content of free volume) leads to faster segmental dynamics of the adsorbed layer, which is even faster than in the neat polymer at higher MW of the adsorbed chains (Fig. 3a). This lower density also leads to lower energy barrier U for restricted segmental fluctuations. As a result, the activation energy estimated from Eq.(8) decreases with increase in MW (Fig. 5b). It is easier for the polymer chains to overcome the potential barrier U at higher temperatures, and this leads to a larger angle of segmental fluctuations. This explains the anomalous increase of $\Delta\varepsilon_{IL}(T)$ with temperature (Fig. 3c) observed in the APL samples. It is alternative explanation to the dead layer model, where it is assumed that number of contributed dipoles into the dielectric response increases at high temperature (unfreezing of dipoles in dead layer). At present, we don't have a microscopic picture that would relate the estimated activation energy (Fig. 5b) to specific polymer parameters, conformations of polymer chains, their density or stretching in the interfacial/adsorbed layer or in the grafted chains.

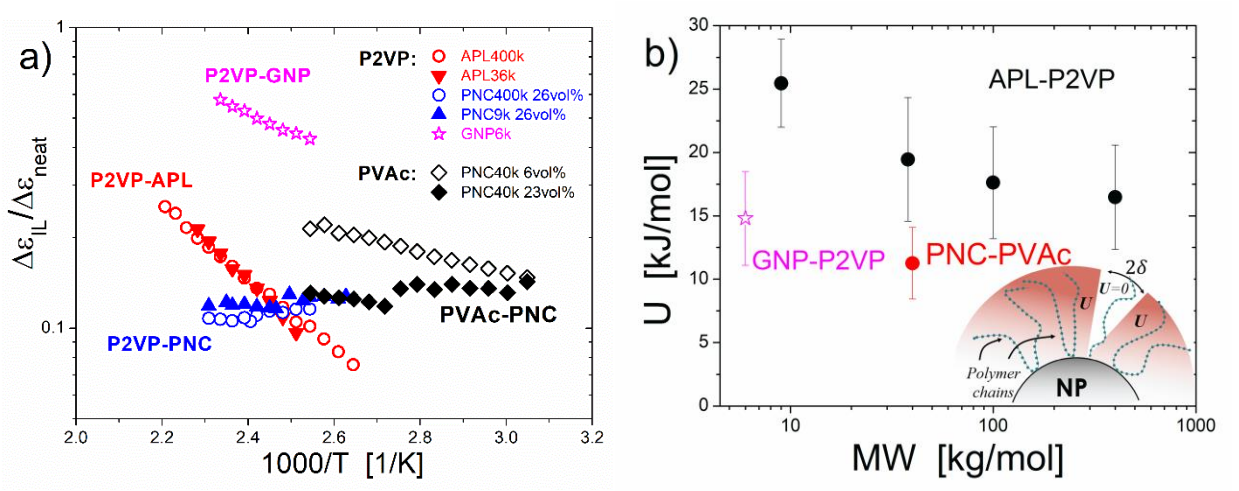

Figure 5. a) Temperature dependence of the ratio $\Delta\varepsilon_{IL}/\Delta\varepsilon_{neat}$ in various APL, PNC and GNP samples. **b)** Molecular weight dependence of the estimated activation energy for adsorbed layer (filled black symbols), for GNP (open magenta star) and PVAc-based PNC with 6vol%

nanoparticles (filled red circle). The cartoon illustrates model assumption for the potential restricting angle fluctuations of a polymer strand, it is zero for conical angle δ, and U for larger angles. For details of the model see SM.

We want to emphasize that detailed BDS studies of thin polymer films revealed that the thickness of the interfacial layer with changed Δε(T) is significantly larger than the thickness of the layer with changed segmental relaxation time [34, 44]. This clearly demonstrates a decoupling in behavior of characteristic time and amplitude of the segmental dynamics in the interfacial region, providing another contradiction to the idea of a 'dead layer'. At the same time this decoupling can be explained by the proposed here mechanism: Effect of specific chain conformation (e.g. chain stretching) induced by an interface can propagate over larger distance, independently of characteristic length scale of changes in segmental relaxation time. Thus, change in Δε can propagate to much longer length scale, while characteristic segmental relaxation time in the interfacial layer is affected not only by chain conformations, but also by polymer-nanoparticles interactions, chain packing, etc., and can be slower or even faster than segmental relaxation in the neat polymer. This decoupling of segmental time scale and amplitude is critical for understanding the interfacial phenomena, and can be one of the reasons for many contradictions in the fields of thin polymer films and PNCs.

It would be important to analyze this effect using neutron scattering spectroscopy that can measure both, time scale and geometry (e.g. mean-squared displacement) of the segmental dynamics. Molecular dynamic simulations might provide even more detailed microscopic insight into this phenomenon. We emphasize that generality of the reduced amplitude of segmental relaxation in PNCs is not obvious. Studied here systems have attractive polymer-nanoparticle interactions.

Whether repulsive interactions will also affect the amplitude of segmental relaxation remains unclear, although example of thin polymer films with amplitude reduced regardless of the polymer-substrate interactions[34, 37, 39, 42, 74] suggests rather general trend.

Conclusion

In summary, the presented here analysis of the dielectric spectra of polymer layer adsorbed to nanoparticles reveals a significant drop in the dielectric strength of segmental dynamics, while characteristic segmental relaxation time remains comparable to that of the neat polymer and even faster. Moreover, the dielectric strength shows anomalous temperature dependence – a decrease upon cooling, in stark contrast to the usual increase with cooling (Curie-law behavior) observed in neat polymers. Similar drop in the dielectric strength of the segmental peak is observed for chains chemically grafted to nanoparticles, in the interfacial layer of regular PNCs [20, 24, 45, 53], and also in thin polymer films [28-31, 33-44]. This effect, however, was not observed in glycerol/silica nanocomposite [84], emphasizing the role of chain connectivity in this phenomenon. We ascribe the observed changes in $\Delta\varepsilon(T)$ to a limited amplitude of segmental fluctuations on the time scale of segmental dynamics. We propose that this reduced amplitude of segmental motions is caused by chain stretching in the interfacial layer or pancake-like structure in the adsorbed layer. It is important to emphasize that depending on the strength of the imposed restrictions on segmental reorientation, the observed temperature dependence of $\Delta\varepsilon(T)$ can be comparable or a bit weaker than in the neat systems, or can even show the anomalous behavior – a decrease of $\Delta\varepsilon(T)$ with cooling.

The obtained results emphasize an interesting new aspect of the dynamics in interfacial and adsorbed polymer layers in PNCs and in thin polymer films. The presence of an interface affects not only characteristic relaxation time, but also the amplitude of segmental motion. Moreover, there is a significant decoupling between the behavior of segmental relaxation time and amplitude in the interfacial region. While the interfacial segmental dynamics can slow down significantly, can be only slightly affected or can be even faster than in the bulk, the amplitude of the segmental fluctuations on the segmental time scale always decreases. This restricted amplitude of segmental mobility and its decoupling from the behavior of characteristic relaxation time might also explain many controversies about dynamics in the interfacial layer, where different conclusions are drawn from different experiments. In all these discussions, possible reduction of the amplitude of segmental dynamics is usually omitted. Detailed microscopic understanding of the mechanism leading to the reduction in segmental dynamics amplitude in the interfacial layer is critical for understanding interfacial phenomena and requires development of an accurate theoretical model.

Acknowledgments

Authors thank Ken Schweizer for many helpful discussions. I.P., B.C. V.B., S.C., A.K., A.P.S acknowledge financial support for materials synthesis (V.B.), dielectric measurements (I.P. B.C. S.C. and A.K.), data analysis (I.P., V.B., A.P.S.) and theoretical model development (I.P. and A.P.S), by the U.S. Department of Energy, Office of Science, Basic Energy Sciences, Materials Sciences and Engineering Division. A.A.Kh. acknowledges the Ministry of Science and Higher Education of the Russian Federation for supporting the research, award # 3.2166.2017/4.6. A.C.G. is thankful for support by the ANR NANODYN project, Grant ANR-14-CE22-0001-01 of the French Agence Nationale de la Recherche.

Supporting Information

TGA curves for the APL systems, Dielectric spectra of the APL systems, Mathematical details of model for temperature dependence of dielectric strength of the adsorbed layer.

Author Information

*__Corresponding author__:

E-mail *sokolov@utk.edu*

References

1. Jancar, J.; Douglas, J.; Starr, F. W.; Kumar, S.; Cassagnau, P.; Lesser, A.; Sternstein, S. S.; Buehler, M., Current issues in research on structure–property relationships in polymer nanocomposites. *Polymer* **2010,** *51* (15), 3321-3343.

2. Balazs, A. C.; Emrick, T.; Russell, T. P., Nanoparticle polymer composites: where two small worlds meet. *Science* **2006,** *314* (5802), 1107-1110.

3. Kumar, S. K.; Benicewicz, B. C.; Vaia, R. A.; Winey, K. I., 50th anniversary perspective: are polymer nanocomposites practical for applications? *Macromolecules* **2017,** *50* (3), 714-731.

4. Baker, R. W.; Low, B. T., Gas separation membrane materials: a perspective. *Macromolecules* **2014,** *47* (20), 6999-7013.

5. Croce, F.; Appetecchi, G.; Persi, L.; Scrosati, B., Nanocomposite polymer electrolytes for lithium batteries. *Nature* **1998,** *394* (6692), 456.

6. Crosby, A. J.; Lee, J. Y., Polymer nanocomposites: the "nano" effect on mechanical properties. *Polymer reviews* **2007,** *47* (2), 217-229.

7. Freeman, B. D., Basis of permeability/selectivity tradeoff relations in polymeric gas separation membranes. *Macromolecules* **1999,** *32* (2), 375-380.

8. Leszczyńska, A.; Njuguna, J.; Pielichowski, K.; Banerjee, J., Polymer/montmorillonite nanocomposites with improved thermal properties: Part I. Factors influencing thermal stability and mechanisms of thermal stability improvement. *Thermochimica Acta* **2007,** *453* (2), 75-96.

9. Mutiso, R. M.; Winey, K. I., Electrical properties of polymer nanocomposites containing rod-like nanofillers. *Progress in Polymer Science* **2015,** *40*, 63-84.

10. Podsiadlo, P.; Kaushik, A. K.; Arruda, E. M.; Waas, A. M.; Shim, B. S.; Xu, J.; Nandivada, H.; Pumplin, B. G.; Lahann, J.; Ramamoorthy, A., Ultrastrong and stiff layered polymer nanocomposites. *Science* **2007,** *318* (5847), 80-83.

11. Ramanathan, T.; Abdala, A.; Stankovich, S.; Dikin, D.; Herrera-Alonso, M.; Piner, R.; Adamson, D.; Schniepp, H.; Chen, X.; Ruoff, R., Functionalized graphene sheets for polymer nanocomposites. *Nature nanotechnology* **2008,** *3* (6), 327.

12. Song, J.; Wang, Y.; Wan, C. C., Review of gel-type polymer electrolytes for lithium-ion batteries. *Journal of Power Sources* **1999,** *77* (2), 183-197.

13. Thakur, V. K.; Gupta, R. K., Recent progress on ferroelectric polymer-based nanocomposites for high energy density capacitors: synthesis, dielectric properties, and future aspects. *Chemical reviews* **2016,** *116* (7), 4260-4317.

14. Tjong, S. C., Structural and mechanical properties of polymer nanocomposites. *Materials Science and Engineering: R: Reports* **2006,** *53* (3-4), 73-197.

15. Merino, S.; Martin, C.; Kostarelos, K.; Prato, M.; Vazquez, E., Nanocomposite hydrogels: 3D polymer–nanoparticle synergies for on-demand drug delivery. *ACS nano* **2015,** *9* (5), 4686-4697.

16. Merkel, T.; Freeman, B.; Spontak, R.; He, Z.; Pinnau, I.; Meakin, P.; Hill, A., Ultrapermeable, reverse-selective nanocomposite membranes. *Science* **2002,** *296* (5567), 519-522.

17. Schadler, L. S.; Kumar, S. K.; Benicewicz, B. C.; Lewis, S. L.; Harton, S. E., Designed interfaces in polymer nanocomposites: A fundamental viewpoint. *MRS bulletin* **2007,** *32* (4), 335-340.

18. Song, Q.; Nataraj, S.; Roussenova, M. V.; Tan, J. C.; Hughes, D. J.; Li, W.; Bourgoin, P.; Alam, M. A.; Cheetham, A. K.; Al-Muhtaseb, S. A., Zeolitic imidazolate framework (ZIF-8) based polymer nanocomposite membranes for gas separation. *Energy & Environmental Science* **2012,** *5* (8), 8359-8369.

19. Xu, H.; Cheng, L.; Wang, C.; Ma, X.; Li, Y.; Liu, Z., Polymer encapsulated upconversion nanoparticle/iron oxide nanocomposites for multimodal imaging and magnetic targeted drug delivery. *Biomaterials* **2011,** *32* (35), 9364-9373.

20. Carroll, B.; Cheng, S. W.; Sokolov, A. P., Analyzing the Interfacial Layer Properties in Polymer Nanocomposites by Broadband Dielectric Spectroscopy. *Macromolecules* **2017,** *50* (16), 6149-6163.

21. Cheng, S. W.; Carroll, B.; Bocharova, V.; Carrillo, J. M. Y.; Sumpter, B. G.; Sokolov, A. P., Structure and dynamics of the interfacial layer in polymer nanocomposites with attractive interactions. *J Chem Phys* **2017,** *146* (20).

22. Senses, E.; Akcora, P., An interface-driven stiffening mechanism in polymer nanocomposites. *Macromolecules* **2013,** *46* (5), 1868-1874.

23. Fragiadakis, D.; Pissis, P.; Bokobza, L., Modified chain dynamics in poly (dimethylsiloxane)/silica nanocomposites. *Journal of non-crystalline solids* **2006,** *352* (42-49), 4969-4972.

24. Holt, A. P.; Bocharova, V.; Cheng, S.; Kisliuk, A. M.; White, B. T.; Saito, T.; Uhrig, D.; Mahalik, J. P.; Kumar, R.; Imel, A. E., Controlling interfacial dynamics: covalent bonding versus physical adsorption in polymer nanocomposites. *ACS nano* **2016,** *10* (7), 6843-6852.

25. Holt, A. P.; Griffin, P. J.; Bocharova, V.; Agapov, A. L.; Imel, A. E.; Dadmun, M. D.; Sangoro, J. R.; Sokolov, A. P., Dynamics at the polymer/nanoparticle interface in poly (2-vinylpyridine)/silica nanocomposites. *Macromolecules* **2014,** *47* (5), 1837-1843.

26. Schönhals, A.; Stauga, R., Broadband dielectric study of anomalous diffusion in a poly(propylene glycol) melt confined to nanopores. *The Journal of Chemical Physics* **1998,** *108* (12), 5130-5136.

27. Fukao, K.; Miyamoto, Y., Glass transitions and dynamics in thin polymer films: Dielectric relaxation of thin films of polystyrene. *Physical Review E* **2000,** *61* (2), 1743-1754.

28. Fukao, K.; Miyamoto, Y., Slow dynamics near glass transitions in thin polymer films. *Physical Review E* **2001,** *64* (1), 011803.

29. Fukao, K.; Uno, S.; Miyamoto, Y.; Hoshino, A.; Miyaji, H., Dynamics of $\ensuremath{\alpha}$ and $\ensuremath{\beta}$ processes in thin polymer films: Poly(vinyl acetate) and poly(methyl methacrylate). *Physical Review E* **2001,** *64* (5), 051807.

30. Labahn, D.; Mix, R.; Schönhals, A., Dielectric relaxation of ultrathin films of supported polysulfone. *Physical Review E* **2009,** *79* (1), 011801.

31. Madkour, S.; Szymoniak, P.; Heidari, M.; von Klitzing, R.; Schönhals, A., Unveiling the Dynamics of Self-Assembled Layers of Thin Films of Poly(vinyl methyl ether) (PVME) by Nanosized Relaxation Spectroscopy. *ACS Applied Materials & Interfaces* **2017,** *9* (8), 7535-7546.

32. Madkour, S.; Yin, H.; Füllbrandt, M.; Schönhals, A., Calorimetric evidence for a mobile surface layer in ultrathin polymeric films: poly(2-vinyl pyridine). *Soft Matter* **2015,** *11* (40), 7942-7952.

33. Martínez-Tong, D. E.; Vanroy, B.; Wübbenhorst, M.; Nogales, A.; Napolitano, S., Crystallization of Poly(l-lactide) Confined in Ultrathin Films: Competition between Finite Size Effects and Irreversible Chain Adsorption. *Macromolecules* **2014,** *47* (7), 2354-2360.

34. Napolitano, S.; Capponi, S.; Vanroy, B., Glassy dynamics of soft matter under 1D confinement: How irreversible adsorption affects molecular packing, mobility gradients and orientational polarization in thin films. *The European Physical Journal E* **2013,** *36* (6), 61.

35. Napolitano, S.; Prevosto, D.; Lucchesi, M.; Pingue, P.; D'Acunto, M.; Rolla, P., Influence of a Reduced Mobility Layer on the Structural Relaxation Dynamics of Aluminum Capped Ultrathin Films of Poly(ethylene terephthalate). *Langmuir* **2007,** *23* (4), 2103-2109.

36. Napolitano, S.; Wübbenhorst, M., The lifetime of the deviations from bulk behaviour in polymers confined at the nanoscale. *Nature communications* **2011,** *2*, 260.

37. Rotella, C.; Napolitano, S.; De Cremer, L.; Koeckelberghs, G.; Wübbenhorst, M., Distribution of Segmental Mobility in Ultrathin Polymer Films. *Macromolecules* **2010,** *43* (20), 8686-8691.

38. Rotella, C.; Napolitano, S.; Vandendriessche, S.; Valev, V. K.; Verbiest, T.; Larkowska, M.; Kucharski, S.; Wübbenhorst, M., Adsorption Kinetics of Ultrathin Polymer Films in the Melt Probed by Dielectric Spectroscopy and Second-Harmonic Generation. *Langmuir* **2011,** *27* (22), 13533-13538.

39. Rotella, C.; Wübbenhorst, M.; Napolitano, S., Probing interfacial mobility profiles via the impact of nanoscopic confinement on the strength of the dynamic glass transition. *Soft Matter* **2011,** *7* (11), 5260-5266.

40. Serghei, A.; Mikhailova, Y.; Eichhorn, K. J.; Voit, B.; Kremer, F., Discrepancies in the characterization of the glass transition in thin films of hyperbranched polyesters. *Journal of Polymer Science Part B: Polymer Physics* **2006,** *44* (20), 3006-3010.

41. Serghei, A.; Mikhailova, Y.; Huth, H.; Schick, C.; Eichhorn, K. J.; Voit, B.; Kremer, F., Molecular dynamics of hyperbranched polyesters in the confinement of thin films. *The European Physical Journal E* **2005,** *17* (2), 199-202.

42. Serghei, A.; Tress, M.; Kremer, F., Confinement Effects on the Relaxation Time Distribution of the Dynamic Glass Transition in Ultrathin Polymer Films. *Macromolecules* **2006,** *39* (26), 9385-9387.

43. Serghei, A.; Tress, M.; Kremer, F., The glass transition of thin polymer films in relation to the interfacial dynamics. *The Journal of Chemical Physics* **2009,** *131* (15), 154904.

44. Yin, H.; Napolitano, S.; Schönhals, A., Molecular Mobility and Glass Transition of Thin Films of Poly(bisphenol A carbonate). *Macromolecules* **2012,** *45* (3), 1652-1662.

45. Cheng, S.; Holt, A. P.; Wang, H.; Fan, F.; Bocharova, V.; Martin, H.; Etampawala, T.; White, B. T.; Saito, T.; Kang, N.-G.; Dadmun, M. D.; Mays, J. W.; Sokolov, A. P., Unexpected molecular weight effect in polymer nanocomposites. *Physical review letters* **2016,** *116* (3), 038302.

46. Baeza, G. P.; Dessi, C.; Costanzo, S.; Zhao, D.; Gong, S.; Alegria, A.; Colby, R. H.; Rubinstein, M.; Vlassopoulos, D.; Kumar, S. K., Network dynamics in nanofilled polymers. *Nature Communications* **2016,** *7* (1), 11368.

47. Harton, S. E.; Kumar, S. K.; Yang, H.; Koga, T.; Hicks, K.; Lee, H.; Mijovic, J.; Liu, M.; Vallery, R. S.; Gidley, D. W., Immobilized Polymer Layers on Spherical Nanoparticles. *Macromolecules* **2010,** *43* (7), 3415-3421.

48. Jiang, N.; Endoh, M. K.; Koga, T.; Masui, T.; Kishimoto, H.; Nagao, M.; Satija, S. K.; Taniguchi, T., Nanostructures and Dynamics of Macromolecules Bound to Attractive Filler Surfaces. *Acs Macro Lett* **2015,** *4* (8), 838-842.

49. Jimenez, A. M.; Zhao, D.; Misquitta, K.; Jestin, J.; Kumar, S. K., Exchange Lifetimes of the Bound Polymer Layer on Silica Nanoparticles. *Acs Macro Lett* **2019,** *8* (2), 166-171.

50. Jouault, N.; Moll, J. F.; Meng, D.; Windsor, K.; Ramcharan, S.; Kearney, C.; Kumar, S. K., Bound Polymer Layer in Nanocomposites. *Acs Macro Lett* **2013,** *2* (5), 371-374.

51. Koga, T.; Barkley, D.; Nagao, M.; Taniguchi, T.; Carrillo, J.-M. Y.; Sumpter, B. G.; Masui, T.; Kishimoto, H.; Koga, M.; Rudick, J. G.; Endoh, M. K., Interphase Structures and Dynamics near Nanofiller Surfaces in Polymer Solutions. *Macromolecules* **2018,** *51* (23), 9462-9470.

52. Cheng, S.; Bocharova, V.; Belianinov, A.; Xiong, S.; Kisliuk, A.; Somnath, S.; Holt, A. P.; Ovchinnikova, O. S.; Jesse, S.; Martin, H.; Etampawala, T.; Dadmun, M.; Sokolov, A. P.,

Unraveling the Mechanism of Nanoscale Mechanical Reinforcement in Glassy Polymer Nanocomposites. *Nano Letters* **2016,** *16* (6), 3630-3637.

53. Genix, A.-C.; Bocharova, V.; Kisliuk, A.; Carroll, B.; Zhao, S.; Oberdisse, J.; Sokolov, A. P., Enhancing the Mechanical Properties of Glassy Nanocomposites by Tuning Polymer Molecular Weight. *ACS Applied Materials & Interfaces* **2018,** *10* (39), 33601-33610.

54. Griffin, P. J.; Bocharova, V.; Middleton, L. R.; Composto, R. J.; Clarke, N.; Schweizer, K. S.; Winey, K. I., Influence of the Bound Polymer Layer on Nanoparticle Diffusion in Polymer Melts. *Acs Macro Lett* **2016,** *5* (10), 1141-1145.

55. Jiang, N.; Wang, J.; Di, X.; Cheung, J.; Zeng, W.; Endoh, M. K.; Koga, T.; Satija, S. K., Nanoscale adsorbed structures as a robust approach for tailoring polymer film stability. *Soft Matter* **2016,** *12* (6), 1801-1809.

56. Jouault, N.; Crawford, M. K.; Chi, C.; Smalley, R. J.; Wood, B.; Jestin, J.; Melnichenko, Y. B.; He, L.; Guise, W. E.; Kumar, S. K., Polymer Chain Behavior in Polymer Nanocomposites with Attractive Interactions. *Acs Macro Lett* **2016,** *5* (4), 523-527.

57. Jouault, N.; Zhao, D.; Kumar, S. K., Role of Casting Solvent on Nanoparticle Dispersion in Polymer Nanocomposites. *Macromolecules* **2014,** *47* (15), 5246-5255.

58. Carroll, B.; Bocharova, V.; Carrillo, J.-M. Y.; Kisliuk, A.; Cheng, S.; Yamamoto, U.; Schweizer, K. S.; Sumpter, B. G.; Sokolov, A. P., Diffusion of Sticky Nanoparticles in a Polymer Melt: Crossover from Suppressed to Enhanced Transport. *Macromolecules* **2018,** *51* (6), 2268-2275.

59. Cheng, S.; Carroll, B.; Lu, W.; Fan, F.; Carrillo, J.-M. Y.; Martin, H.; Holt, A. P.; Kang, N.-G.; Bocharova, V.; Mays, J. W., Interfacial properties of polymer nanocomposites: Role of chain rigidity and dynamic heterogeneity length scale. *Macromolecules* **2017,** *50* (6), 2397-2406.

60. Jouault, N.; Jestin, J., Intra-and Interchain Correlations in Polymer Nanocomposites: A Small-Angle Neutron Scattering Extrapolation Method. *Acs Macro Lett* **2016,** *5* (10), 1095-1099.

61. Gong, S. S.; Chen, Q.; Moll, J. F.; Kumar, S. K.; Colby, R. H., Segmental Dynamics of Polymer Melts with Spherical Nanoparticles. *Acs Macro Lett* **2014,** *3* (8), 773-777.

62. Kremer, F. S., A. , *Broadband Dielectric Spectroscopy*. Springer-Verlag: Berlin, 2002.

63. Boucher, V. M.; Cangialosi, D.; Alegrìa, A.; Colmenero, J.; González-Irun, J.; Liz-Marzan, L. M., Physical aging in PMMA/silica nanocomposites: enthalpy and dielectric relaxation. *Journal of Non-Crystalline Solids* **2011,** *357* (2), 605-609.

64. Füllbrandt, M.; Purohit, P. J.; Schönhals, A., Combined FTIR and dielectric investigation of poly (vinyl acetate) adsorbed on silica particles. *Macromolecules* **2013,** *46* (11), 4626-4632.

65. Holt, A. P., The Effect of Attractive Polymer-Nanoparticle Interactions on the Local Segmental Dynamics of Polymer Nanocomposites. **2016**.

66. Klonos, P. A.; Goncharuk, O. V.; Pakhlov, E. M.; Sternik, D.; Deryło-Marczewska, A.; Kyritsis, A.; Gun'ko, V. M.; Pissis, P., Morphology, Molecular Dynamics, and Interfacial Phenomena in Systems Based on Silica Modified by Grafting Polydimethylsiloxane Chains and Physically Adsorbed Polydimethylsiloxane. *Macromolecules* **2019,** *52* (7), 2863-2877.

67. Carrillo, J.-M. Y.; Cheng, S.; Kumar, R.; Goswami, M.; Sokolov, A. P.; Sumpter, B. G., Untangling the Effects of Chain Rigidity on the Structure and Dynamics of Strongly Adsorbed Polymer Melts. *Macromolecules* **2015,** *48* (12), 4207-4219.

68. Hanakata, P. Z.; Douglas, J. F.; Starr, F. W., Interfacial mobility scale determines the scale of collective motion and relaxation rate in polymer films. *Nature Communications* **2014,** *5* (1), 4163.

69. Pazmiño Betancourt, B. A.; Douglas, J. F.; Starr, F. W., Fragility and cooperative motion in a glass-forming polymer–nanoparticle composite. *Soft Matter* **2013,** *9* (1), 241-254.

70. Zhang, W.; Starr, F. W.; Douglas, J. F., Collective Motion in the Interfacial and Interior Regions of Supported Polymer Films and Its Relation to Relaxation. *The Journal of Physical Chemistry B* **2019,** *123* (27), 5935-5941.

71. Guiselin, O., Irreversible Adsorption of a Concentrated Polymer Solution. *Europhysics Letters (EPL)* **1992,** *17* (3), 225-230.

72. Hao, N.; Böhning, M.; Schönhals, A., Dielectric Properties of Nanocomposites Based on Polystyrene and Polyhedral Oligomeric Phenethyl-Silsesquioxanes. *Macromolecules* **2007,** *40* (26), 9672-9679.

73. Casalini, R.; Roland, C. M., Local and Global Dynamics in Polypropylene Glycol/Silica Composites. *Macromolecules* **2016,** *49* (3), 3919-3924.

74. Napolitano, S.; Wübbenhorst, M., Dielectric Signature of a Dead Layer in Ultrathin Films of a Nonpolar Polymer. *The Journal of Physical Chemistry B* **2007,** *111* (31), 9197-9199.

75. Fragiadakis, D.; Pissis, P.; Bokobza, L., Glass transition and molecular dynamics in poly (dimethylsiloxane)/silica nanocomposites. *Polymer* **2005,** *46* (16), 6001-6008.

76. Sargsyan, A.; Tonoyan, A.; Davtyan, S.; Schick, C., The amount of immobilized polymer in PMMA SiO2 nanocomposites determined from calorimetric data. *European Polymer Journal* **2007,** *43* (8), 3113-3127.

77. Iijima, M.; Kamiya, H., Layer-by-Layer Surface Modification of Functional Nanoparticles for Dispersion in Organic Solvents. *Langmuir* **2010,** *26* (23), 17943-17948.

78. Kamiya, H.; Suzuki, H.; Kato, D.; Jimbo, G., Densification of Alkoxide-Derived Fine Silica Powder Compact by Ultra-High-Pressure Cold Isostatic Pressing. *J Am Ceram Soc* **1993,** *76* (1), 54-64.

79. Tyagi, M.; Casalini, R.; Roland, C. M., Short time and structural dynamics in polypropylene glycol nanocomposite. *Rubber Chemistry and Technology* **2017,** *90* (2), 264-271.

80. Chehrazi, E.; Taheri Qazvini, N., Nanoconfined segmental dynamics in miscible polymer blend nanocomposites: the influence of the geometry of nanoparticles. *Iranian Polymer Journal* **2013,** *22* (8), 613-622.

81. Pandis, C.; Logakis, E.; Kyritsis, A.; Pissis, P.; Vodnik, V. V.; Džunuzović, E.; Nedeljković, J. M.; Djoković, V.; Rodríguez Hernández, J. C.; Gómez Ribelles, J. L., Glass transition and polymer dynamics in silver/poly(methyl methacrylate) nanocomposites. *European Polymer Journal* **2011,** *47* (8), 1514-1525.

82. Batistakis, C.; Lyulin, A. V.; Michels, M. A. J., Slowing Down versus Acceleration in the Dynamics of Confined Polymer Films. *Macromolecules* **2012,** *45* (17), 7282-7292.

83. Fröhlich, H., *Theory of dielectrics : dielectrics constant and dielectric loss*. 2nd ed.; Clarendon Press: Oxford, 1986; p vi, 192 p.

84. Cheng, S.; Mirigian, S.; Carrillo, J.-M. Y.; Bocharova, V.; Sumpter, B. G.; Schweizer, K. S.; Sokolov, A. P., Revealing spatially heterogeneous relaxation in a model nanocomposite. *The Journal of chemical physics* **2015,** *143* (19), 194704.

85. de Gennes, P. G., Conformations of Polymers Attached to an Interface. *Macromolecules* **1980,** *13* (5), 1069-1075.

86. Liu, G.; Cheng, H.; Yan, L.; Zhang, G., Study of the Kinetics of the Pancake-to-Brush Transition of Poly(N-isopropylacrylamide) Chains. *The Journal of Physical Chemistry B* **2005,** *109* (47), 22603-22607.

87. Ou-Yang, H. D.; Gao, Z., A pancake-to-brush transition in polymer adsorption. *J. Phys. II France* **1991,** *1* (11), 1375-1385.

88. Poling-Skutvik, R.; Olafson, K. N.; Narayanan, S.; Stingaciu, L.; Faraone, A.; Conrad, J. C.; Krishnamoorti, R., Confined Dynamics of Grafted Polymer Chains in Solutions of Linear Polymer. *Macromolecules* **2017,** *50* (18), 7372-7379.